Chapter 2

REVIEW AND COMPARISON OF THREE THIN FILM INSTABILITY MODELS

As mentioned above in Ch. 1, nanofilms on a heated substrate are found experimentally to be unstable. To better understand this phenomenon, several groups have approached this process theoretically by modeling it as a fluid instability. All of the proposed mechanisms for this phenomenon revolve around thin film hydrodynamic instability theory. They differ in the specific driving force which destabilizes the film against the force of surface tension but possess several unifying features. In this chapter we review the three proposed mechanisms and synthesize the previous work into one derivation which has consistent notation and serves to highlight the origin and influence of the various driving forces. We also present the derived expressions which the later experimental results are compared with in Ch. 3, Ch. 4, and Ch. 5.

The remainder of this chapter is organized as follows. In Sec. 2.1, a thin film height evolution equation is derived for the position of the nanofilm/air interface, $h(x, y, t)$, starting from the basic equations of fluid mechanics. Subsequently in Sec. 2.2 these equations are nondimensionalized and simplified using the long wavelength approximation. Then in Sec. 2.3 linear stability analysis is applied for each of the three proposed models. The results of the linear stability analysis give tangible predictions for the wavelength and growth rate of the fastest growing mode.

2.1 Fluid Dynamics Governing Equations

To specify the system completely, we define the domain, the governing equations, and the boundary conditions for the system. As mentioned in Ch. 1, the system of interest is a free surface molten nanofilm bounded by an air layer. Note that this derivation is only concerned with the fluid dynamics of the liquid nanofilm and not the air layer. Due to the large difference between the density and viscosity of the liquid nanofilm and the density and viscosity of the air layer only the dynamics of the fluid layer are explicitly considered.

2.1.1 Nanofilm Instability Geometry

The domain which we will consider is a thin liquid film which has an initial height h_o. This can also be interchangeably referred to as the film thickness. The film is

Figure 2.1: Schematic of the instability geometry

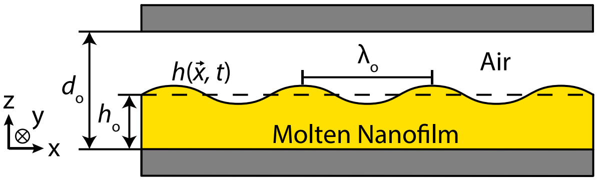

The molten nanofilm is bounded from below by a heated substrate and from above by a plate which is cooled. The total plate separation is denoted by d_o, while the initial film thickness is denoted by h_o. The temperature drop from hot to cold plates is denoted by $\Delta T = T_H - T_C$ and the lateral spacing of the protrusions is denoted by λ_o.

supported from below by a rigid, impermeable, heated substrate. The upper surface of the film is a free interface and a distance d_o from the bottom of the film there exists a cooled, upper plate which constrains the system in the vertical direction.

2.1.2 Mass and Momentum Continuity Equations

There are two differential equations which we will use to describe this system. The first differential equation is the mass continuity equation. We will assume incompressible flow and the resulting equation is

$$\nabla \cdot \vec{u} = 0. \tag{2.1}$$

In this equation $\vec{u} = (u, v, w)$ is the velocity of the molten nanofilm as a function of space and time. The other differential equation which governs the fluid dynamics in the molten layer is the Navier-Stokes equation where we have assumed that the fluid is Newtonian. This equation physically represents the conservation of momentum and has the form

$$\rho \frac{D\vec{u}}{Dt} = -\boldsymbol{\nabla} p + \mu \boldsymbol{\nabla}^2 \vec{u} + \vec{f}_{\text{body}}, \tag{2.2}$$

where ρ is the density of the fluid, p is the pressure, μ is the shear viscosity and $\vec{f}_{\text{body}}$ is the effect of body forces on the fluid. The most common body force which acts on fluids is gravity. Previous theoretical work [8–10] has estimated that gravity is negligible in nanofilm experiments due to the minuscule height scales. As such, f_{body} will be set to zero for the remainder of this work. The notation for the time derivative on the left hand side of the equation is the convective, or material, derivative and is defined by

$$\frac{D}{Dt} \equiv \frac{\partial}{\partial t} + \vec{u} \cdot \boldsymbol{\nabla}. \tag{2.3}$$

This describes how a quantity changes in time as well as local changes due to variations along the local velocity field.

2.1.3 Fluid Velocity and Pressure Boundary Conditions

With the governing equations specified, we now outline the boundary conditions required for solution of $\vec{u}$ and p. At the bottom of the liquid layer ($z = 0$ in Fig. 2.1) there is a no-slip and impenetrability condition with the solid wall

$$\vec{u}(z = 0) = 0. \tag{2.4}$$

At the free interface there is both a kinematic boundary condition and an interfacial stress balance. The kinematic boundary condition relates the vertical component of the fluid velocity to the change of the film height at the interface

$$w(z = h) = \frac{\partial h}{\partial t} + \vec{u}_{||} \cdot \boldsymbol{\nabla}_{||} h. \tag{2.5}$$

The subscript || denotes that only the $\hat{x}$ and $\hat{y}$ components of the subscripted quantity should be included in the expressions. Consequently, the horizontal velocity is defined by

$$\vec{u}_{||} \equiv u\hat{x} + v\hat{y}. \tag{2.6}$$

Similarly, the horizontal gradient, $\boldsymbol{\nabla}_{||}$, is composed of the derivatives solely in the $\hat{x}$ and $\hat{y}$ directions. In other words,

$$\boldsymbol{\nabla}_{||} = \hat{x}\frac{\partial}{\partial x} + \hat{y}\frac{\partial}{\partial y}. \tag{2.7}$$

Beyond the kinematic boundary condition, we must balance the normal and tangential stresses at the interface which can be encapsulated in the following equation which applies at $z = h(x, y, t)$

$$(\mathbf{T}_{\text{air}} - \mathbf{T}_{\text{film}}) \cdot \hat{n} + p_{\text{ac}}\hat{n} + p_{\text{el}}\hat{n} + \boldsymbol{\nabla}_s \gamma - \gamma \hat{n} \left(\boldsymbol{\nabla}_s \cdot \hat{n}\right) = 0. \tag{2.8}$$

In this equation the stress tensors, $\mathbf{T}$, are subscripted by their respective layers and will be described in detail below. The unit normal vector, $\hat{n}$, is perpendicular to the nanofilm surface everywhere and points from the film to the air. The terms p_{ac} and p_{el} are pressures arising from acoustic or electrical sources, respectively, and will be defined in the relevant sections below since they correspond to specific proposed models. These have been explicitly removed from the fluid pressure p in the stress tensor so that limiting cases can be considered for each model. Additionally, γ is the surface tension at the air/film interface and $\boldsymbol{\nabla}_s$ is the surface gradient which is defined by

$$\boldsymbol{\nabla}_s \equiv \boldsymbol{\nabla} - \hat{n}(\hat{n} \cdot \boldsymbol{\nabla}). \tag{2.9}$$

This means that the surface gradient operator only exists in the plane of the interface, by definition, since the normal components have been removed. Furthermore, note that $\boldsymbol{\nabla}_s = \boldsymbol{\nabla}_{\|}$ only where the interface is flat and $\hat{n} = \hat{z}$.

2.2 Scaling the Governing Equations and Applying the Lubrication Approximation

The system of interest has been defined and now the governing equations are scaled to simplify the analysis. In particular, we know that both the overall system dimensions and the characteristic lateral length scale of the instability growth, λ_o, are much larger than the initial film thickness, h_o. As such, we define a small quantity

$$\epsilon \equiv \frac{h_o}{\lambda_o}, \tag{2.10}$$

and after scaling the equations we only keep terms to first order in ϵ since $\epsilon^2 \ll 1$. This approximation has several names including the lubrication or long wavelength approximation [17–19]. All the horizontal lengths are scaled by λ_o and all the vertical lengths scaled by h_o. Time is scaled using the horizontal length and a characteristic lateral speed, u_c, which can be chosen arbitrarily. Therefore,

$$X = \frac{x}{\lambda_o}; Y = \frac{y}{\lambda_o}, \tag{2.11}$$

$$Z = \frac{z}{h_o}; H = \frac{h}{h_o}; D = \frac{d}{h_o}, \tag{2.12}$$

$$U = \frac{u}{u_c}; V = \frac{v}{u_c}; W = \frac{w}{w_c}, \tag{2.13}$$

$$\tau = \frac{t u_c}{\lambda_o}; P = \frac{p}{P_c}; \Gamma = \frac{\gamma}{\Gamma_c}, \tag{2.14}$$

$$\widetilde{\boldsymbol{\nabla}_s} = \lambda_o \boldsymbol{\nabla}_s; \widetilde{\boldsymbol{\nabla}_{\|}} = \lambda_o \boldsymbol{\nabla}_{\|}. \tag{2.15}$$

The scalings for the pressure, P_c, and surface tension, Γ_c, will be determined below during the simplification of the Navier-Stokes equations. The quantity w_c is a characteristic velocity scale for flow in the vertical direction. Due to the disparate length scales, it would not be correct to scale all the fluid velocities by the same quantity. Now we return to the governing equations and scale them using the quantities above which will illuminate several relationships between these quantities and allow us to simplify the equations significantly.

The first equation we will scale is the continuity equation to get a relationship between u_c and w_c. Scaling Eq. (2.1) results in

$$\frac{\partial U}{\partial X} + \frac{\partial V}{\partial Y} + \frac{w_c}{\epsilon u_c}\frac{\partial W}{\partial Z} = 0.$$

To ensure that all the terms in the continuity equation are of the same order the vertical velocity scale is set by $w_c = \epsilon u_c$. Consequently, the scaled continuity equation is

$$\frac{\partial U}{\partial X} + \frac{\partial V}{\partial Y} + \frac{\partial W}{\partial Z} = 0. \tag{2.16}$$

Using these velocity scalings, the Navier-Stokes equations are simplified. For simplicity, the equations are resolved into components during the scaling process. These are

$$\begin{aligned}
\hat{x} : \epsilon Re\frac{DU}{D\tau} &= -\frac{\epsilon h_o P_c}{\mu u_c}\frac{\partial P}{\partial X} + \epsilon^2\frac{\partial^2 U}{\partial X^2} + \epsilon^2\frac{\partial^2 U}{\partial Y^2} + \frac{\partial^2 U}{\partial Z^2},\\
\hat{y} : \epsilon Re\frac{DV}{D\tau} &= -\frac{\epsilon h_o P_c}{\mu u_c}\frac{\partial P}{\partial Y} + \epsilon^2\frac{\partial^2 V}{\partial X^2} + \epsilon^2\frac{\partial^2 V}{\partial Y^2} + \frac{\partial^2 V}{\partial Z^2},\\
\hat{z} : \epsilon^3 Re\frac{DW}{D\tau} &= -\frac{\epsilon h_o P_c}{\mu u_c}\frac{\partial P}{\partial Z} + \epsilon^2\left(\epsilon^2\frac{\partial^2 W}{\partial X^2} + \epsilon^2\frac{\partial^2 W}{\partial Y^2} + \frac{\partial^2 W}{\partial Z^2}\right).
\end{aligned}$$

In these equations, the Reynolds number, Re, has been defined as

$$Re = \frac{\rho u_c h_o}{\mu}. \tag{2.17}$$

The Reynolds number represents the ratio of inertial forces to viscous forces within the fluid [19]. Based on the similarity of the terms in front of the pressure in each of the three components, there is a clear scaling for the pressure

$$P_c = \frac{\mu u_c}{\epsilon h_o}. \tag{2.18}$$

With this definition for the nondimensionalization of the pressure, the long wavelength approximation is now implemented which requires that (1) $\epsilon^2 \ll 1$ and (2) $\epsilon Re \ll 1$. This approximation takes advantage of the disparity between vertical and lateral length scales to greatly reduce the complexity of the analysis. Neglecting terms of second order in ϵ or higher, the scaled Navier-Stokes equations are

$$\| : \frac{\partial^2 \vec{U}_\|}{\partial Z^2} = \widetilde{\boldsymbol{\nabla}}_\| P, \tag{2.19}$$

$$\hat{z} : \frac{\partial P}{\partial Z} = 0. \tag{2.20}$$

Moving on to the boundary conditions, the no-slip and impenetrability condition from Eq. (2.4) scales in a straightforward manner

$$\vec{U}(Z = 0) = 0. \tag{2.21}$$

Similarly, the kinematic boundary condition from Eq. (2.5) becomes

$$W(Z = H) = \frac{\partial H}{\partial \tau} + \vec{U}_{\|}(Z = H) \cdot \boldsymbol{\nabla}_{\|} H. \tag{2.22}$$

Scaling the interfacial stress balance in Eq. (2.8) within the long wavelength approximation is more complicated and intermediate results will first be derived and then compiled into the final expression. Specifically the normal vector, $\hat{n}$, the surface gradient, $\boldsymbol{\nabla}_s$, the surface divergence of the normal vector, $\boldsymbol{\nabla}_s \cdot \hat{n}$, and the stress tensor, $\mathbf{T}_i$, are scaled.

2.2.1 Scaling the Normal Vector to a Surface

The surface of the film described by $h(x, y)$ can be expressed in three dimensions as a locus of points where a function F is equal to zero.

$$F(x, y, z) = z - h(x, y) = 0.$$

The unit normal to the surface is found by taking the gradient of F and normalizing it

$$\hat{n} = \frac{\boldsymbol{\nabla} F}{|\boldsymbol{\nabla} F|} = \left(\left(\frac{\partial h}{\partial x} \right)^2 + \left(\frac{\partial h}{\partial y} \right)^2 + 1 \right)^{-1/2} \left(-\frac{\partial h}{\partial x} \hat{x} - \frac{\partial h}{\partial y} \hat{y} + \hat{z} \right). \tag{2.23}$$

Each of these quantities scales as defined above, so the terms in the preceding square root will be of order ϵ^2 and will be neglected in this analysis. Consequently, the scaled unit normal in nondimensional units becomes

$$\hat{n} = -\epsilon \widetilde{\boldsymbol{\nabla}_{\|}} H + \hat{Z}. \tag{2.24}$$

2.2.2 Scaling the Surface Gradient Operator

We can now take the scaled normal vector in Eq. (2.24) and use it to compute the scaled surface gradient, $\widetilde{\boldsymbol{\nabla}_s}$. Recalling the definition of the surface gradient in Eq. (2.9), this expression scales to

$$\widetilde{\boldsymbol{\nabla}_s} = \widetilde{\boldsymbol{\nabla}} - \hat{n} \left(\hat{n} \cdot \widetilde{\boldsymbol{\nabla}} \right).$$

After substitution of the normal vector from Eq. (2.23) into the definition of the surface gradient in Eq. (2.9), scaling the resulting expression, and simplifying, the scaled surface gradient becomes

$$\widetilde{\boldsymbol{\nabla}_s} = \widetilde{\boldsymbol{\nabla}_\parallel} + \left(\widetilde{\boldsymbol{\nabla}_\parallel} H\right)\frac{\partial}{\partial Z} + \hat{Z}\epsilon\left(\widetilde{\boldsymbol{\nabla}_\parallel} H\right)\left(\widetilde{\boldsymbol{\nabla}_\parallel} + \left(\widetilde{\boldsymbol{\nabla}_\parallel} H\right)\frac{\partial}{\partial Z}\right). \tag{2.25}$$

Note that in this equation the derivatives grouped with H within parentheses only act on H, not on the argument of the surface gradient operator itself.

2.2.3 Scaling the Surface Divergence of the Normal Vector

The last term in the stress balance from Eq. (2.8) represents the effect of surface tension and depends on the surface divergence of the normal vector. Since these two quantities have been scaled in Eq. (2.9) and Eq. (2.24), they are combined to find

$$\widetilde{\boldsymbol{\nabla}_s} \cdot \hat{n} = -\epsilon \widetilde{\boldsymbol{\nabla}_\parallel^2} H. \tag{2.26}$$

When computing this expression, we note that none of the quantities in the normal vector shown in Eq. (2.24) depend on Z.

2.2.4 Scaling the Stress Tensor

The stress tensors in the film and air layers are crucial pieces of the interfacial stress balance in Eq. (2.8). Within each layer i, the stress tensor takes the form

$$\mathbf{T}_i = -p_i \mathbf{I} + 2\mu_i \mathbf{E}_i. \tag{2.27}$$

Here p_i is the fluid pressure and $\mathbf{E}_i$ is the rate of strain tensor. Since the viscosity of air is many orders of magnitude smaller than the viscosity of the molten nanofilm, the product $2\mu_{\text{air}}\mathbf{E}_{\text{air}}$ will be neglected as a small contribution. The subscripts on μ_{film} and E_{film} will be dropped since there can be no confusion. The rate of strain tensor is defined by

$$\mathbf{E} \equiv \frac{1}{2}\left(\boldsymbol{\nabla}\vec{u} + \left(\boldsymbol{\nabla}\vec{u}\right)^{\text{tr}}\right) = \frac{1}{2}\begin{bmatrix} 2\dfrac{\partial u}{\partial x} & \dfrac{\partial u}{\partial y} + \dfrac{\partial v}{\partial x} & \dfrac{\partial u}{\partial z} + \dfrac{\partial w}{\partial x} \\ \dfrac{\partial v}{\partial x} + \dfrac{\partial u}{\partial y} & 2\dfrac{\partial v}{\partial y} & \dfrac{\partial v}{\partial z} + \dfrac{\partial w}{\partial y} \\ \dfrac{\partial w}{\partial x} + \dfrac{\partial u}{\partial z} & \dfrac{\partial w}{\partial y} + \dfrac{\partial v}{\partial z} & 2\dfrac{\partial w}{\partial z} \end{bmatrix}. \tag{2.28}$$

In the stress balance of Eq. (2.8), the quantity which enters the equation is the stress tensor difference dotted with the normal vector, $\hat{n}$. From the definition of the stress tensor in Eq. (2.27) one obvious scaling for the stress tensor is the characteristic pressure, P_c. Therefore,

$$\frac{1}{P_c}\left(\mathbf{T}_{\text{air}} - \mathbf{T}_{\text{film}}\right)\cdot\hat{n} = \frac{p_{\text{air}} - p_{\text{film}}}{P_c}\hat{n} - \frac{2\mu}{P_c}\mathbf{E}\cdot\hat{n}.$$

Note that $p_{\text{air}} - p_{\text{film}} = p$. Additionally, converting the rate of strain tensor to nondimensional units, dotting by the normal vector on the right, and dropping terms of order ϵ^2 yields

$$\frac{2\mu}{P_c}\mathbf{E}\cdot\hat{n} = \epsilon\begin{bmatrix} 2\epsilon\frac{\partial U}{\partial X} & \epsilon\frac{\partial U}{\partial Y} + \epsilon\frac{\partial V}{\partial X} & \frac{\partial U}{\partial Z} \\ \epsilon\frac{\partial V}{\partial X} + \epsilon\frac{\partial U}{\partial Y} & 2\epsilon\frac{\partial V}{\partial Y} & \frac{\partial V}{\partial Z} \\ \frac{\partial U}{\partial Z} & \frac{\partial V}{\partial Z} & 2\epsilon\frac{\partial W}{\partial Z} \end{bmatrix}\begin{bmatrix} -\epsilon\frac{\partial H}{\partial X} \\ -\epsilon\frac{\partial H}{\partial Y} \\ 1 \end{bmatrix} = \epsilon\frac{\partial\vec{U}_{\parallel}}{\partial Z}.$$

Inserting these results above yields

$$\frac{1}{P_c}\left(\mathbf{T}_{\text{air}} - \mathbf{T}_{\text{film}}\right)\cdot\hat{n} = P\hat{n} - \epsilon\frac{\partial\vec{U}_{\parallel}}{\partial Z}. \tag{2.29}$$

All the intermediary results in Eqs. (2.24), (2.25), (2.26), and (2.29) are inserted back into the full stress balance in Eq. (2.8) to find

$$P\hat{n} - \epsilon\frac{\partial\vec{U}_{\parallel}}{\partial Z} + P_{\text{ac}}\hat{n} + P_{\text{el}}\hat{n} + \frac{\Gamma_c}{\lambda_o P_c}\widetilde{\boldsymbol{\nabla}}_s\Gamma + \frac{\epsilon\Gamma_c}{\lambda_o P_c}\Gamma\left(\widetilde{\boldsymbol{\nabla}_{\parallel}^2}H\right)\hat{n} = 0.$$

Note that this equation contains both normal and tangential components. This equation now suggests a natural scaling for Γ_c so that all the tangential components (the second and the fifth terms above) will be of order ϵ and all the vertical components will be of order unity

$$\Gamma_c = \epsilon\lambda_o P_c = \frac{\mu u_c}{\epsilon}. \tag{2.30}$$

The nondimensionalized surface tension has the form reminiscent of the traditional capillary number, Ca, [19] except scaled by a factor of ϵ^{-3}. As such, the modified capillary number is defined as

$$\overline{Ca} = \frac{1}{\epsilon^2\Gamma} = \frac{\mu u_c}{\gamma\epsilon^3} = \frac{Ca}{\epsilon^3}. \tag{2.31}$$

The capillary number represents the ratio of viscous forces to forces due to surface tension. Similar to the way that we split the vectorial Navier-Stokes equations into vertical and horizontal components in Eqs. (2.19) and (2.20), the interfacial stress balance is decomposed into components

$$\parallel : \frac{\partial \vec{U}_{\parallel}}{\partial Z} = -\widetilde{\boldsymbol{\nabla}}_s \Gamma, \tag{2.32}$$

$$\hat{z} : P = -\frac{1}{\overline{Ca}} \left(\widetilde{\boldsymbol{\nabla}}^2_{\parallel} H \right) - P_{\text{ac}} - P_{\text{el}}. \tag{2.33}$$

2.2.5 Summary of Scaled Equations

The governing equations and the boundary conditions have all been scaled to transform them into nondimensional equations which were then simplified using the lubrication approximation. For convenience, here are all the scaled equations which will be referenced when deriving the thin film height evolution equation

$$\frac{\partial U}{\partial X} + \frac{\partial V}{\partial Y} + \frac{\partial W}{\partial Z} = 0, \tag{2.34}$$

$$\frac{\partial^2 \vec{U}_{\parallel}}{\partial Z^2} = \widetilde{\boldsymbol{\nabla}}_{\parallel} P, \tag{2.35}$$

$$\frac{\partial P}{\partial Z} = 0, \tag{2.36}$$

$$\vec{U}(Z = 0) = 0, \tag{2.37}$$

$$W(Z = H) = \frac{\partial H}{\partial \tau} + \vec{U}_{\parallel} \cdot \boldsymbol{\nabla}_{\parallel} H, \tag{2.38}$$

$$\frac{\partial \vec{U}_{\parallel}(Z = H)}{\partial Z} = -\widetilde{\boldsymbol{\nabla}}_s \Gamma, \tag{2.39}$$

$$P(Z = H) = -\frac{1}{\overline{Ca}} \left(\widetilde{\boldsymbol{\nabla}}^2_{\parallel} H \right) - P_{\text{ac}}(Z = H) - P_{\text{el}}(Z = H). \tag{2.40}$$

2.2.6 Thin Film Height Evolution Equation

To proceed from these equations to a single differential equation for the interface evolution, the general approach will be to use the kinematic boundary condition to introduce a temporal derivative of $H(X, Y, \tau)$ and then rewrite everything in terms of $H(X, Y, \tau)$. Note that the interface height is both a function of time and position. For notational convenience, we will drop this explicit functional dependence in the following equations. To do this, consider a slightly rewritten form of the continuity equation in Eq. (2.34) (or equivalently Eq. (2.16))

$$\widetilde{\boldsymbol{\nabla}}_{\parallel} \cdot \vec{U}_{\parallel} + \frac{\partial W}{\partial Z} = 0.$$

Integrating this equation with respect to Z from $Z = 0$ to $Z = H$ results in

$$W(Z = H) - W(Z = 0) + \int_0^H \widetilde{\boldsymbol{\nabla}}_{\|} \cdot \vec{U}_{\|} dZ = 0.$$

The first term is the kinematic boundary condition from Eq. (2.38) (or equivalently Eq. (2.22)) and the second is the impenetrability condition from Eq. (2.37) (or equivalently Eq. (2.21)). After substitution this equation becomes

$$\frac{\partial H}{\partial \tau} + \vec{U}_{\|}(Z = H) \cdot \widetilde{\boldsymbol{\nabla}}_{\|} H + \int_0^H \widetilde{\boldsymbol{\nabla}}_{\|} \cdot \vec{U}_{\|} dZ = \frac{\partial H}{\partial \tau} + \widetilde{\boldsymbol{\nabla}}_{\|} \cdot \int_0^H \vec{U}_{\|} dZ = 0. \quad (2.41)$$

In the second equality the Leibnitz rule for differentiation has been used to bring the derivative outside the integral [19]. All that remains now is to solve for $\vec{U}_{\|}$ and then integrate the result to find the height evolution equation. To accomplish this, the remaining equations are used. From the vertical component of the scaled Navier-Stokes equations in Eq. (2.36) (or equivalently Eq. (2.20)), it is clear that the pressure, P, is independent of the vertical coordinate. As such, the lateral components of the scaled Navier-Stokes equations in Eq. (2.35) (or equivalently Eq. (2.19)) are integrated twice to solve for

$$\vec{U}_{\|} = \frac{Z^2}{2} \widetilde{\boldsymbol{\nabla}}_{\|} P + A_{\|} Z + B_{\|}. \quad (2.42)$$

In this equation, $A_{\|}$ and $B_{\|}$ are two component vectors which are the integration constants for each component equation. Based on the no-slip condition from Eq. (2.37) (or equivalently, Eq. (2.21)) it follows that $B_{\|} = 0$. The other integration constant can be determined by using the horizontal components of the interfacial stress balance in Eq. (2.39) (or equivalently Eq. (2.32)). Since this poses a condition on the derivative of the horizontal velocity at $Z = H$, the velocity which satisfies this equation is clearly

$$\vec{U}_{\|} = \left(\frac{Z^2}{2} - HZ \right) \widetilde{\boldsymbol{\nabla}}_{\|} P - Z \widetilde{\boldsymbol{\nabla}}_s \Gamma.$$

The horizontal gradient of the pressure can be computed from the vertical component of the interfacial stress balance in Eq. (2.40) (or equivalently Eq. (2.33)). If we insert this expression for the gradient of the pressure into the preceding equation we find that

$$\vec{U}_{\|} = \left(\frac{Z^2}{2} - HZ \right) \left(\frac{-1}{Ca} \left(\widetilde{\boldsymbol{\nabla}}_{\|}^3 H \right) - \widetilde{\boldsymbol{\nabla}}_{\|} P_{\text{ac}}(Z = H) - \widetilde{\boldsymbol{\nabla}}_{\|} P_{\text{el}}(Z = H) \right) - Z \widetilde{\boldsymbol{\nabla}}_s \Gamma.$$

As mentioned previously, the specific forms of P_{ac}, P_{el}, and $\widetilde{\boldsymbol{\nabla}}_s\Gamma$ depend on the chosen model and will be discussed further below. Regardless, none of these values depend on Z and the evaluation at $Z = H$ will be suppressed from now on. Consequently, this equation for the horizontal velocity can be integrated from $Z = 0$ to $Z = H$ to find

$$\int_0^H \vec{U}_{\parallel} dZ = \frac{H^3}{3}\left(\frac{1}{\overline{Ca}}\left(\widetilde{\boldsymbol{\nabla}}_{\parallel}^3 H\right) + \widetilde{\boldsymbol{\nabla}}_{\parallel} P_{\text{ac}} + \widetilde{\boldsymbol{\nabla}}_{\parallel} P_{\text{el}}\right) - \frac{H^2}{2}\widetilde{\boldsymbol{\nabla}}_s\Gamma. \tag{2.43}$$

Inserting Eq. (2.43) back into Eq. (2.41) yields the height evolution equation

$$\frac{\partial H}{\partial \tau} + \widetilde{\boldsymbol{\nabla}}_{\parallel} \cdot \left[\frac{H^3}{3}\left(\frac{1}{\overline{Ca}}\left(\widetilde{\boldsymbol{\nabla}}_{\parallel}^3 H\right) + \widetilde{\boldsymbol{\nabla}}_{\parallel} P_{\text{ac}} + \widetilde{\boldsymbol{\nabla}}_{\parallel} P_{\text{el}}\right) - \frac{H^2}{2}\widetilde{\boldsymbol{\nabla}}_s\Gamma\right] = 0. \tag{2.44}$$

2.3 Linear Stability Analysis

While the exact forms for P_{ac}, P_{el}, and $\widetilde{\boldsymbol{\nabla}}_s\Gamma$ have not been specified yet, it will be shown below they all depend exclusively on H. As such, through the chain rule the derivatives will act on H and therefore any constant H will satisfy this differential equation. To investigate the stability of this family of solutions, the initially flat interface (denoted by $H = 1$) is perturbed by a function of the form

$$H = 1 + \widetilde{\delta h} e^{\beta(K)\tau} e^{i\vec{K}_{\parallel}\cdot\vec{X}_{\parallel}}. \tag{2.45}$$

The quantity $\widetilde{\delta h}$ is the magnitude of the perturbation and is assumed to be small so that we neglect terms of second order in this quantity. The real exponential contains the nondimensional growth rate, β, and the imaginary exponential contains explicit dependence on the horizontal wavevector, $\vec{K}_{\parallel}$, which contains only $\hat{x}$ and $\hat{y}$ components. The magnitude of the wavevector is related to the real space wavelength, λ, by

$$K = |\vec{K}_{\parallel}| = \frac{2\pi\lambda_o}{\lambda}. \tag{2.46}$$

The nondimensional growth rate, β, is related to the dimensional growth rate, b, through

$$\beta(K) = \frac{b(k)\lambda_o}{u_c}. \tag{2.47}$$

To proceed any further with the linearization, the forms of each model will be specified separately in turn.

Figure 2.2: Instability geometry in SC model

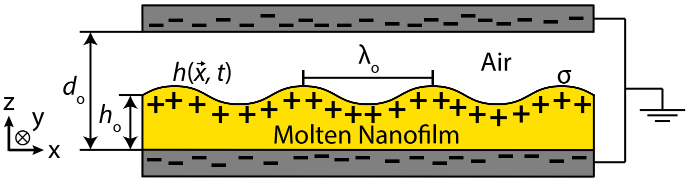

The distinguishing feature of the SC model is the presence of a surface charge density, σ, along the interface which induces an electric field that leads to the destabilizing electric pressure.

2.3.1 SC Model: Electrostatic Pressure

Within the SC model the driving force is posited to be electrostatic in origin. In the work of Chou and Zhuang [2, 3], there was assumed to be a surface charge density along the interface which would induce image charges in the upper and lower bounding plates which were grounded, as illustrated in Fig. 2.2. The presence of the electric charges creates an electric field which they hypothesized was responsible for the deformation of the interface. Because the AP model had not yet been published by Schäffer *et al.*, the net pressure from acoustic phonon reflections is zero and so $P_{\rm ac} = 0$. Furthermore, they did not consider the surface tension to vary with any external field which implies that $\widetilde{\boldsymbol{\nabla}}_s\Gamma = 0$. All that remains is to define the electric pressure, $P_{\rm el}$, created by the interfacial charge density and complete the linear stability analysis.

The electrostatic pressure arises from the difference between the Maxwell stress tensors, $\mathbf{T}_i^{\rm em}$, in the air and nanofilm layers. Explicitly, the magnitude of the pressure in the normal direction is

$$P_{\rm el} = \frac{1}{P_c}\hat{n}\cdot\left(\mathbf{T}^{\rm em}_{\rm air} - \mathbf{T}^{\rm em}_{\rm film}\right)\cdot\hat{n}. \tag{2.48}$$

The Maxwell stress tensor in matter without any magnetic fields has the form [20]

$$\mathbf{T}^{\rm em} = \vec{E}\vec{D} - \frac{1}{2}\mathbf{I}\left(\vec{E}\cdot\vec{D}\right), \tag{2.49}$$

where $\vec{E}$ is the electric field and $\vec{D} = \varepsilon_o\varepsilon\vec{E}$ is the electric displacement field. ε_o is the the permittivity of free space. Note that ε is the relative permittivity of the medium, and is distinct from ϵ which is the long-wavelength expansion parameter. In air we assume that the relative permittivity is equal to unity, so that $\varepsilon_{\rm air} = 1$. To proceed further, the electric fields in both the air and film layers are solved using Laplace's equation and then the Maxwell stress tensors are computed. These are then inserted into the electrostatic pressure term, P_{el}. Once P_{el} has been computed, linear stability analysis is applied to the resulting thin film height evolution equation to find the wavevector and growth rate of the fastest growing mode.

Electrostatic Governing Equations

Within the derivation of Chou and Zhuang, it was assumed that there are no significant magnetic fields present in the system. This reduces the problem of solving for the electric field within the system to a simple electrostatics problem. Furthermore, it was assumed that there was no volumetric charge density present within either the air or film layers and that the only charge is present at the interface between the two layers. The interfacial charge density is constant during deformation and denoted by σ. These assumptions imply that the governing differential equation is Laplace's equation

$$\boldsymbol{\nabla}^2 \phi_i = 0. \tag{2.50}$$

In this expression ϕ_i is the potential in the ith layer. Since there is no externally applied voltage in this system, both the upper and lower bounding plates are assumed to be grounded so that

$$\phi_{\text{film}}(z = 0) = 0, \tag{2.51}$$

$$\phi_{\text{air}}(z = d) = 0. \tag{2.52}$$

Along the interface, the usual electrostatic boundary conditions are applied [20]

$$\hat{n} \cdot \left(\vec{D}_{\text{air}} - \vec{D}_{\text{film}}\right) = \varepsilon_o \hat{n} \cdot \left(\vec{E}_{\text{air}} - \varepsilon_{\text{film}} \vec{E}_{\text{film}}\right) = \sigma, \tag{2.53}$$

$$\hat{n} \times \left(\vec{E}_{\text{air}} - \vec{E}_{\text{film}}\right) = 0. \tag{2.54}$$

Finally, the relationship between the electric field and the electric potential is

$$\vec{E}_i = -\boldsymbol{\nabla} \phi_i. \tag{2.55}$$

Scaled Electrostatic Equations

To scale the electrostatic equations, the same scalings which were defined in Sec. 2.2 are used but there are two more for the electric potential and the electric field.

$$\widetilde{\phi}_i = \frac{\phi_i}{\Phi_c}; \widetilde{\vec{E}}_i = \frac{\vec{E}_i h_o}{\Phi_c}. \tag{2.56}$$

The quantity Φ_c is a characteristic potential which will be determined in the course of scaling the equations, similar to how P_c and Γ_c were determined above. The relationship between the nondimensional electric potential and electric field transforms from Eq. (2.55) to

$$\widetilde{\vec{E}}_i = -\epsilon \widetilde{\boldsymbol{\nabla}}_{\|} \widetilde{\phi}_i - \frac{\partial \widetilde{\phi}_i}{\partial Z}. \tag{2.57}$$

Once we nondimensionalize Laplace's equation from Eq. (2.50) we find that to second order

$$\frac{\partial \widetilde{\phi}_i}{\partial Z^2} = 0. \tag{2.58}$$

The exterior Dirichlet boundary conditions simply become

$$\widetilde{\phi}_{\text{film}}(Z = 0) = 0, \tag{2.59}$$

$$\widetilde{\phi}_{\text{air}}(Z = D) = 0. \tag{2.60}$$

The tangential electrostatic boundary condition of Eq. (2.54) is equivalent to the requirement that the potential be continuous across the interface. Therefore,

$$\widetilde{\phi}_{\text{film}}(Z = H) = \widetilde{\phi}_{\text{air}}(Z = H). \tag{2.61}$$

The final electrostatic boundary equation is the one shown in Eq. (2.53) for the normal components of the electric displacement field at the interface. Using the scaled normal vector which was derived above in Eq. (2.24), this yields

$$\frac{\Phi_c \varepsilon_o}{h_o}\left(-\epsilon \widetilde{\boldsymbol{\nabla}}_{\|} H + \hat{Z}\right) \cdot \left(-\epsilon \widetilde{\boldsymbol{\nabla}}_{\|} \widetilde{\phi}_{\text{air}} - \varepsilon_o \frac{\partial \widetilde{\phi}_{\text{air}}}{\partial Z} \hat{Z} + \epsilon \varepsilon_{\text{film}} \widetilde{\boldsymbol{\nabla}}_{\|} \widetilde{\phi}_{\text{film}} + \varepsilon_{\text{film}} \frac{\partial \widetilde{\phi}_{\text{film}}}{\partial Z} \hat{Z}\right) = \sigma.$$

From this it is clear that all the tangential terms in this equation are order ϵ^2 and can be neglected. Furthermore, the characteristic electric potential scale arises from the charge density at the interface and should be

$$\Phi_c = \frac{\sigma h_o}{\varepsilon_o}. \tag{2.62}$$

This boundary condition then simplifies to

$$\varepsilon_{\text{film}} \frac{\partial \widetilde{\phi}_{\text{film}}(Z = H)}{\partial Z} - \frac{\partial \widetilde{\phi}_{\text{air}}(Z = H)}{\partial Z} = 1. \tag{2.63}$$

Electric Field Solution

The scaled Laplace equation from Eq. (2.58) was integrated twice with respect to Z, yielding electric potentials in each layer that are linear.

$$\begin{aligned}\widetilde{\phi}_{\text{film}} &= A^{\text{SC}}_{\text{film}} Z + B^{\text{SC}}_{\text{film}},\\ \widetilde{\phi}_{\text{air}} &= A^{\text{SC}}_{\text{air}} Z + B^{\text{SC}}_{\text{air}}.\end{aligned}$$

In this equation $A^{\text{SC}}_{\text{film}}$, $B^{\text{SC}}_{\text{film}}$, $A^{\text{SC}}_{\text{air}}$, and $B^{\text{SC}}_{\text{air}}$ are integration constants. The Dirichlet boundary conditions on the bounding plates from Eqs. (2.59) and (2.60) imply that $B^{\text{SC}}_{\text{film}} = 0$ and $B^{\text{SC}}_{\text{air}} = -DA^{\text{SC}}_{\text{air}}$

$$\begin{aligned}\widetilde{\phi}_{\text{film}} &= A^{\text{SC}}_{\text{film}} Z,\\ \widetilde{\phi}_{\text{air}} &= A^{\text{SC}}_{\text{air}} (Z - D).\end{aligned}$$

The electric potential must be continuous across $Z = H$ according to the boundary condition in Eq. (2.61), so that $A^{\text{SC}}_{\text{film}}$ can be expressed in terms of $A^{\text{SC}}_{\text{air}}$

$$A^{\text{SC}}_{\text{film}} = A^{\text{SC}}_{\text{air}} \frac{(H - D)}{H}.$$

This implies that the electric potentials should have the form

$$\begin{aligned}\widetilde{\phi}_{\text{film}} &= A^{\text{SC}}_{\text{air}} \frac{Z(H - D)}{H},\\ \widetilde{\phi}_{\text{air}} &= A^{\text{SC}}_{\text{air}} (Z - D).\end{aligned}$$

The only remaining boundary condition is Eq. (2.63) and this implies that the one remaining integration constant is

$$A^{\text{SC}}_{\text{air}} = \frac{H}{(\varepsilon_{\text{film}} - 1) H - \varepsilon_{\text{film}} D}.$$

Returning to the electric potentials, they have the form

$$\widetilde{\phi}_{\text{film}} = \frac{Z(H - D)}{(\varepsilon_{\text{film}} - 1) H - \varepsilon_{\text{film}} D}, \tag{2.64}$$

$$\widetilde{\phi}_{\text{air}} = \frac{H(Z - D)}{(\varepsilon_{\text{film}} - 1) H - \varepsilon_{\text{film}} D}. \tag{2.65}$$

Based on the relation in Eq. (2.57) between the electric potential and the electric field, the nondimensional electric fields at the interface are

$$\widetilde{\vec{E}}_{\text{film}} = \epsilon \left(\frac{DH\widetilde{\boldsymbol{\nabla}}_{\parallel} H}{\left[\varepsilon_{\text{film}} D - (\varepsilon_{\text{film}} - 1)\, H\right]^2} \right) - \frac{(D - H)}{\varepsilon_{\text{film}} D - (\varepsilon_{\text{film}} - 1)\, H} \hat{Z}, \tag{2.66}$$

$$\widetilde{\vec{E}}_{\text{air}} = \epsilon \left(\frac{\varepsilon_{\text{film}} D(H - D)\widetilde{\boldsymbol{\nabla}}_{\parallel} H}{\left[\varepsilon_{\text{film}} D - (\varepsilon_{\text{film}} - 1)\, H\right]^2} \right) - \frac{H}{\varepsilon_{\text{film}} D - (\varepsilon_{\text{film}} - 1)\, H} \hat{Z}. \tag{2.67}$$

The most important thing to note about these electric fields is that the vertical components do not have an ϵ, while the horizontal components are first order in ϵ. This means that when these electric fields are inserted into the Maxwell stress tensor, all terms which contain products with two tangential components, such as $E_x E_y$, $E_x E_x$, and $E_y E_y$, are order ϵ^2 and can be neglected. Computing the expression for the normal component of the stress tensor dotted into the normal vector yields

$$\hat{n} \cdot \mathbf{T}^{\text{em}} \cdot \hat{n} = \varepsilon_o \varepsilon \begin{bmatrix} -\epsilon \frac{\partial H}{\partial X} & -\epsilon \frac{\partial H}{\partial Y} & 1 \end{bmatrix} \begin{bmatrix} -\frac{1}{2} E_z^2 & 0 & E_x E_z \\ 0 & -\frac{1}{2} E_z^2 & E_y E_z \\ E_x E_z & E_y E_z & \frac{1}{2} E_z^2 \end{bmatrix} \begin{bmatrix} -\epsilon \frac{\partial H}{\partial X} \\ -\epsilon \frac{\partial H}{\partial Y} \\ 1 \end{bmatrix} = \frac{\varepsilon_o \varepsilon}{2} E_z^2.$$

Recalling the form of the electric pressure from Eq. (2.48), the electric pressure is

$$P_{\text{el}} = \frac{\varepsilon_o}{2P_c} \left(E_{\text{air},z}^2 - \varepsilon_{\text{film}} E_{\text{film},z}^2 \right).$$

In terms of the electric fields which are expressed in Eqs. (2.66) and (2.67), this pressure becomes

$$P_{\text{el}} = \frac{\sigma^2}{2\varepsilon_o P_c} \left(\frac{(1 - \varepsilon_{\text{film}}) H^2 + 2\varepsilon_{\text{film}} DH - \varepsilon_{\text{film}} D^2}{\left[\varepsilon_{\text{film}} D - (\varepsilon_{\text{film}} - 1)\, H\right]^2} \right). \tag{2.68}$$

Linear Stability Predictions

Returning to the height evolution equation in Eq. (2.44), the gradient of the electrostatic pressure was computed and substituted yielding the following expression

$$\frac{\partial H}{\partial \tau} + \widetilde{\boldsymbol{\nabla}}_{\parallel} \cdot \left[\frac{H^3}{3\overline{Ca}} \left(\widetilde{\boldsymbol{\nabla}}_{\parallel}^3 H \right) + \frac{H^3 \sigma^2}{3\varepsilon_o P_c} \left(\frac{\varepsilon_{\text{film}} D^2}{\left[\varepsilon_{\text{film}} D - (\varepsilon_{\text{film}} - 1)\, H\right]^3} \right) \widetilde{\boldsymbol{\nabla}}_{\parallel} H \right] = 0. \tag{2.69}$$

Insertion of the linear stability perturbation function from Eq. (2.45) and cancellation of the common exponentials yields a nondimensional dispersion relation where terms of order $\widetilde{\delta h}^2$ have been dropped

$$\beta^{\mathrm{SC}}(K) + \frac{K^4}{3\overline{Ca}} - \frac{\sigma^2}{3\varepsilon_o P_c}\left(\frac{\varepsilon_{\mathrm{film}} D^2}{[\varepsilon_{\mathrm{film}} D - (\varepsilon_{\mathrm{film}} - 1)]^3}\right) K^2 = 0. \tag{2.70}$$

This specific dispersion relation has a representative form that will be borne out in the other proposed models. The dispersion relations for each model are of the general form

$$\beta(K) = A_2 K^2 - A_4 K^4, \tag{2.71}$$

where A_2 and A_4 are constants whose exact form depends on the model. As such, the location and magnitude of the maximum growth rate can be found from this general form. The mode with the maximum growth rate is assumed to be the one observed experimentally so the wavevector at which this maximum occurs should then correspond to the characteristic wavelength of the real space pattern which is observed. The form of the dispersion relation in Eq. (2.71) can be solved analytically for the wavevector corresponding to the maximum growth rate. This maximum wavevector is denoted by K_o

$$K_o = \sqrt{\frac{A_2}{2A_4}}. \tag{2.72}$$

The maximum value of the growth rate is then

$$\beta_o \equiv \beta(K_o) = \frac{A_2^2}{4A_4}. \tag{2.73}$$

For the SC model, A_2 and A_4 are

$$A_2^{\mathrm{SC}} = \frac{\sigma^2}{3\varepsilon_o P_c}\left(\frac{\varepsilon_{\mathrm{film}} D^2}{[\varepsilon_{\mathrm{film}} D - (\varepsilon_{\mathrm{film}} - 1)]^3}\right), \tag{2.74}$$

$$A_4^{\mathrm{SC}} = \frac{1}{3\overline{Ca}}. \tag{2.75}$$

Consequently, K_o and β_o for the SC model are

$$K_o^{\mathrm{SC}} = \sqrt{\frac{\sigma^2 h_o D^2}{2\varepsilon_o \varepsilon_{\mathrm{film}}^2 \gamma \epsilon^2}}\left(D + \frac{1}{\varepsilon_{\mathrm{film}}} - 1\right)^{-3/2}, \tag{2.76}$$

$$\beta_o^{\mathrm{SC}} = \frac{\lambda_o h_o}{3\mu u_c \gamma}\left(\frac{\sigma^2 D^2}{2\varepsilon_o \varepsilon_{\mathrm{film}}^2}\right)^2 \left(D + \frac{1}{\varepsilon_{\mathrm{film}}} - 1\right)^{-6}. \tag{2.77}$$

Figure 2.3: Instability geometry in AP model

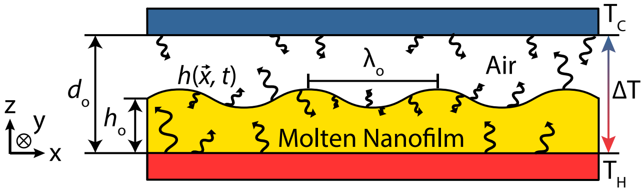

The distinguishing feature of the AP model is the coherent propagation of acoustic phonons through the bilayers, which create a destabilizing radiation pressure.

These are the same quantities as those derived by Zhuang [3], just expressed in nondimensional terms. The dimensional quantities will be presented in Sec. 2.3.4 with the results from the other two models.

2.3.2 AP Model: Acoustic Phonon Radiation Pressure

As opposed to the SC model which relies on electric fields, the driving instability mechanism in both the AP and TC models is a thermal one. The AP model was derived by Schäffer and co-workers [4–6] and they assumed that phonon reflections from all the interfaces in the system would sum to create a net pressure, P_{ac}, which acted as a destabilizing force on the interface. They did not consider the surface tension to vary with any external field which implies that $\widetilde{\boldsymbol{\nabla}}_s \Gamma = 0$, as in the SC model. They did not expect any charge density to be present in the system and did not apply an external voltage, so they did not include any electric effects and therefore $P_{\text{el}} = 0$. To derive an expression for P_{ac}, the temperature in the system was computed from which the thermal flux through the system was calculated. The heat flux was then substituted into the acoustic phonon radiation pressure.

Within the AP model, Schäffer and co-workers assumed that the magnitude of the acoustic phonon pressure was

$$p_{\text{AP}} = -\frac{2\overline{Q}}{u_p}|\vec{q}|, \tag{2.78}$$

where $\vec{q}$ is the heat flux density, u_p is the speed of sound in the molten nanofilm, and $\overline{Q}$ is the acoustic quality factor. A microscopic derivation of $\overline{Q}$ was published [4, 6], but in their subsequent analysis it has been treated as a fitting parameter during analysis of experimental data. To proceed further with their derivation, the governing thermal equations are defined, scaled, and then solved to find the temperature in the system. From the temperature in the system the heat flux through the bilayers is calculated and then substituted into the acoustic phonon radiation pressure. The acoustic phonon radiation pressure is then substituted into the height evolution equation, and linear stability analysis is performed to find the maximum growth rate and its corresponding wavevector for the AP model.

Thermal Governing Equations

There are two differential equations which govern the temperature in the system. The first is Fourier's law of thermal conduction:

$$\vec{q} = -k\boldsymbol{\nabla}\mathrm{T}. \tag{2.79}$$

In this expression, k is thermal conductivity and T is the temperature. The second is the equation describing the conservation of heat

$$\rho c_p \frac{D\mathrm{T}}{Dt} = -\boldsymbol{\nabla} \cdot \vec{q}. \tag{2.80}$$

The quantity c_p is the specific heat capacity. These two equations were combined using a simple substitution and the assumption that the thermal conductivities of each layer in the system are constant and isotropic. This assumption allows the resulting equation to be written as the usual heat equation

$$\rho c_p \frac{D\mathrm{T}}{Dt} = k\boldsymbol{\nabla}^2\mathrm{T}. \tag{2.81}$$

For boundary conditions, the bottom surface of the nanofilm was assumed to be isothermal at a temperature $\mathrm{T_H}$ while the top surface of the air layer was assumed to be isothermal at a temperature $\mathrm{T_C}$ with $\mathrm{T_H} > \mathrm{T_C}$. Finally, both temperature and heat flux density must be continuous at the interface. In total, these requirements are summarized in the following set of equations

$$\mathrm{T}_{\mathrm{film}}(z = 0) = \mathrm{T_H}, \tag{2.82}$$

$$\mathrm{T}_{\mathrm{air}}(z = d) = \mathrm{T_C}, \tag{2.83}$$

$$\mathrm{T}_{\mathrm{film}}(z = h) = \mathrm{T}_{\mathrm{air}}(z = h), \tag{2.84}$$

$$-k_{\mathrm{film}}\boldsymbol{\nabla}\mathrm{T}_{\mathrm{film}}(z = h) = -k_{\mathrm{air}}\boldsymbol{\nabla}\mathrm{T}_{\mathrm{air}}(z = h). \tag{2.85}$$

Scaled Thermal Equations

To scale these equations only one new scaling is needed in addition to the ones contained in Sec. 2.2. This scaling is for the temperature

$$\Theta \equiv \frac{\mathrm{T} - \mathrm{T_C}}{\mathrm{T_H} - \mathrm{T_C}} = \frac{\mathrm{T} - \mathrm{T_C}}{\Delta \mathrm{T}}, \tag{2.86}$$

where Θ is the nondimensional temperature and $\Delta\mathrm{T} \equiv \mathrm{T_H} - \mathrm{T_C}$ is the temperature drop between the bounding plates. The utility of this scaling will become apparent when the isothermal boundary conditions are scaled. First, the heat equation in Eq. (2.81) becomes

$$\epsilon Pr Re \frac{D\Theta}{D\tau} = \epsilon^2 \left(\frac{\partial^2 \Theta}{\partial X^2} + \frac{\partial^2 \Theta}{\partial Y^2} \right) + \frac{\partial^2 \Theta}{\partial Z^2}.$$

In this expression an additional dimensionless number has been defined in addition to the Reynolds number, Re, which was defined in Eq. (2.17). This new number is the Prandtl number, Pr, and has the form

$$Pr = \frac{c_p \mu}{k}. \tag{2.87}$$

The Prandtl number reflects the ratio of the viscous diffusion of momentum to the thermal diffusivity. On the size scales relevant to experiment, the product $\epsilon Pr Re$ is small [8–10], so the temporal dependence of the left half of Eq. (2.87) will be neglected in addition to the terms of order ϵ^2. It becomes

$$\frac{\partial^2 \Theta}{\partial Z^2} = 0. \tag{2.88}$$

The boundary conditions have the following scalings

$$\Theta_{\text{film}}(Z = 0) = 1, \tag{2.89}$$

$$\Theta_{\text{air}}(Z = D) = 0, \tag{2.90}$$

$$\Theta_{\text{film}}(Z = H) = \Theta_{\text{air}}(Z = H), \tag{2.91}$$

$$\widetilde{\boldsymbol{\nabla}} \Theta_{\text{film}}(Z = H) = \kappa \widetilde{\boldsymbol{\nabla}} \Theta_{\text{air}}(Z = H). \tag{2.92}$$

In the last equation the quantity $\kappa \equiv k_{\text{air}}/k_{\text{film}}$ has been defined as the thermal conductivity ratio.

Temperature Field Solution

The scaled heat equation was integrated directly in both the film and air layers to yield

$$\begin{aligned}\Theta_{\text{film}} &= A^{\text{AP}}_{\text{film}} Z + B^{\text{AP}}_{\text{film}},\\ \Theta_{\text{air}} &= A^{\text{AP}}_{\text{air}} Z + B^{\text{AP}}_{\text{air}}.\end{aligned}$$

As in the SC model section, $A^{\text{AP}}_{\text{film}}$, $B^{\text{AP}}_{\text{film}}$, $A^{\text{AP}}_{\text{air}}$, and $B^{\text{AP}}_{\text{air}}$ are integration constants. The two Dirichlet boundary conditions in Eqs. (2.89) and (2.90) imply that $B^{\text{AP}}_{\text{film}} = 1$ and $B^{\text{AP}}_{\text{air}} = -DA^{\text{AP}}_{\text{air}}$ such that

$$\begin{aligned}\Theta_{\text{film}} &= A^{\text{AP}}_{\text{film}} Z + 1,\\ \Theta_{\text{air}} &= A^{\text{AP}}_{\text{air}} (Z - D).\end{aligned}$$

From Eq. (2.91) the continuity of temperature requires that

$$A^{\text{AP}}_{\text{air}} = \frac{A^{\text{AP}}_{\text{film}} H + 1}{H - D}.$$

Then the temperatures in each layer must be of the form

$$\begin{aligned}\Theta_{\text{film}} &= A^{\text{AP}}_{\text{film}} Z + 1,\\ \Theta_{\text{air}} &= \left(A^{\text{AP}}_{\text{film}} H + 1\right) \frac{Z - D}{H - D}.\end{aligned}$$

The final boundary condition is the continuity of thermal flux in Eq. (2.92). This determines the last constant to be

$$A^{\text{AP}}_{\text{film}} = \frac{-\kappa}{D + (\kappa - 1) H}.$$

Consequently, the nondimensional temperature in each layer is

$$\Theta_{\text{film}} = \frac{D - H + \kappa (H - Z)}{D + (\kappa - 1) H}, \tag{2.93}$$

$$\Theta_{\text{air}} = \frac{D - Z}{D + (\kappa - 1) H}. \tag{2.94}$$

Based on these expressions, the magnitude of the thermal flux density will be in the $\hat{Z}$ direction to first order in ϵ. This implies that the nondimensional acoustic phonon pressure at the interface is

$$P_{\text{AP}} = -\frac{2\overline{Q} k_{\text{air}} \Delta \text{T}}{u_p P_c h_o} \frac{\partial \Theta_{\text{air}}}{\partial Z} = \frac{2\overline{Q} k_{\text{air}} \Delta \text{T}}{u_p P_c h_o} \left(\frac{1}{D + (\kappa - 1) H}\right). \tag{2.95}$$

Linear Stability Predictions

Returning to the height evolution equation in Eq. (2.44), the horizontal gradient of the acoustic phonon pressure was computed and substituted to yield the following height evolution equation for the AP mode

$$\frac{\partial H}{\partial \tau} + \widetilde{\boldsymbol{\nabla}}_{\parallel} \cdot \left[\frac{H^3}{3\overline{Ca}} \left(\widetilde{\boldsymbol{\nabla}}_{\parallel}^3 H \right) + \frac{2\overline{Q} k_{\text{air}} \Delta \text{T} H^3}{3 u_p P_c h_o} \left(\frac{1-\kappa}{[D + (\kappa - 1) H]^2} \right) \widetilde{\boldsymbol{\nabla}}_{\parallel} H \right] = 0. \quad (2.96)$$

Once again the perturbation function from Eq. (2.45) was inserted into the height evolution equation to find the dispersion relation for the AP model

$$\beta^{\text{AP}}(K) + \frac{K^4}{3\overline{Ca}} - \frac{2\overline{Q} k_{\text{air}} \Delta \text{T}}{3 u_p P_c h_o} \left(\frac{1-\kappa}{[D + \kappa - 1]^2} \right) K^2 = 0. \quad (2.97)$$

The general forms for K_o and β_o that were derived in Eq. (2.72) and Eq. (2.73) yield the wavevector and growth after association of the constants

$$A_2^{\text{AP}} = \frac{2\overline{Q} k_{\text{air}} \Delta \text{T}}{3 u_p P_c h_o} \left(\frac{1-\kappa}{[D + \kappa - 1]^2} \right), \quad (2.98)$$

$$A_4^{\text{AP}} = \frac{1}{3\overline{Ca}}. \quad (2.99)$$

The nondimensional values of K_o^{AP} and β_o^{AP} are

$$K_o^{\text{AP}} = \sqrt{\frac{\overline{Q} k_{\text{air}} (1-\kappa) \Delta \text{T}}{\gamma u_p \epsilon^2}} \, (D + \kappa - 1)^{-1}, \quad (2.100)$$

$$\beta_o^{\text{AP}} = \frac{L}{3 \gamma \mu u_c h_o} \left(\frac{\overline{Q} k_{\text{air}} (1-\kappa) \Delta \text{T}}{u_p} \right)^2 (D + \kappa - 1)^{-4}. \quad (2.101)$$

Once again, these are the same quantities as those derived by Schäffer and coworkers [4–6], just expressed in nondimensional terms. The dimensional quantities will be presented in Sec. 2.3.4 with the results from the other two models.

2.3.3 TC Model: Thermocapillary Shear

The TC model is similar to the AP model in that the driving force for the instability is thermal, but it has a different origin for the destabilizing force. The AP model defines a destabilizing pressure acting normal to the interface while in the TC model the force is a shear tangential to the interface. This tangential shear arises from differences in surface tension which occur due to the temperature variations along

Figure 2.4: Instability geometry in TC model

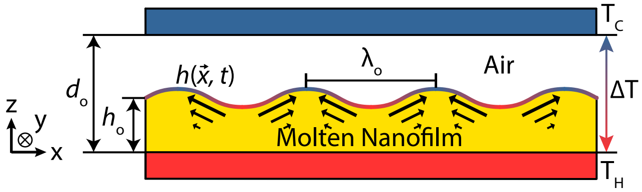

The distinguishing feature of the TC model is variation of surface tension with temperature that drives a destabilizing thermocapillary shear.

the interface. Within this model, originally posited by Dietzel and Troian [8–10], the dominant force arises from the $\widetilde{\nabla}_s\Gamma$ term while the pressure terms from the other two models, P_{ac} and P_{el}, are both equal to zero. The derivation of this model is relatively shorter than those of the SC and AP models because the temperature field throughout the system has already been computed in Sec. 2.3.2 and the scaled results from Eq. (2.93) and Eq. (2.94) port over directly.

When computing the $\widetilde{\nabla}_s\Gamma$ term, Dietzel and Troian assumed that the surface tension only depends on temperature and that the surface tension depends linearly on temperature. This implies that the surface gradient of the surface tension is

$$\widetilde{\nabla}_s\Gamma = \frac{\Delta \mathrm{T}}{\Gamma_c}\frac{\partial\gamma}{\partial \mathrm{T}}\widetilde{\nabla}_s\Theta = -\frac{\epsilon\gamma_T\Delta \mathrm{T}}{\mu u_c}\widetilde{\nabla}_s\Theta. \tag{2.102}$$

In this expression the thermocapillary coefficient, γ_T, was defined as

$$\gamma_{\mathrm{T}} = -\left|\frac{\partial\gamma}{\partial \mathrm{T}}\right|. \tag{2.103}$$

The minus sign has been explicitly brought out to the front of this equation since for single component fluids, this quantity must always be negative. The quantity in front of the gradient is a scaled Marangoni number [19], which represents the ratio of surface tension forces to viscous forces. It was defined by

$$\overline{Ma} \equiv \frac{\epsilon\gamma_{\mathrm{T}}\Delta \mathrm{T}}{\mu u_c} = \epsilon Ma. \tag{2.104}$$

From here, the temperature at the interface was substituted from either Eq. (2.93) or Eq. (2.94). From the continuity of temperature at the interface they must have the same value at $Z = H$. Then we take the surface gradient to find

$$\widetilde{\nabla}_s\Gamma = -\frac{\kappa D\overline{Ma}}{\left[D + (\kappa - 1)\, H\right]^2}\left(\widetilde{\nabla}_{\|}H + \epsilon\left(\widetilde{\nabla}_{\|}H\right)^2\hat{Z}\right). \tag{2.105}$$

The $\hat{Z}$ components in this expression are second order in ϵ when $\widetilde{\boldsymbol{\nabla}_s}\Gamma$ is substituted into the scaled interfacial stress balance from Eq. (2.30). Consequently, they do not appear below.

Linear Stability Predictions

Substitution of the surface gradient of the surface tension from Eq. (2.105) into the height evolution equation from Eq. (2.44) yields

$$\frac{\partial H}{\partial \tau} + \widetilde{\boldsymbol{\nabla}}_\parallel \cdot \left[\frac{H^3}{3\overline{Ca}} \left(\widetilde{\boldsymbol{\nabla}}^3_\parallel H \right) + \frac{H^2 \kappa D \overline{Ma}}{2\left[D + (\kappa - 1) H \right]^2} \widetilde{\boldsymbol{\nabla}}_\parallel H \right] = 0. \tag{2.106}$$

In this case the dispersion relation is

$$\beta^{\mathrm{TC}}(K) + \frac{K^4}{3\overline{Ca}} - \frac{\kappa D \overline{Ma}}{2\left[D + \kappa - 1 \right]^2} K^2 = 0. \tag{2.107}$$

For the TC model the dispersion relation constants are

$$A_2^{\mathrm{TC}} = \frac{\kappa D \overline{Ma}}{2\left[D + \kappa - 1 \right]^2}, \tag{2.108}$$

$$A_4^{\mathrm{TC}} = \frac{1}{3\overline{Ca}}. \tag{2.109}$$

This then implies that the values of K_o^{TC} and β_o^{TC} are

$$K_o^{\mathrm{TC}} = \sqrt{\frac{3\kappa\gamma_\mathrm{T}\Delta\mathrm{T}}{4\gamma\epsilon^2}} \left(\sqrt{D} + \frac{\kappa - 1}{\sqrt{D}} \right)^{-1}, \tag{2.110}$$

$$\beta_o^{\mathrm{TC}} = \frac{3L}{\gamma\mu u_c h_o} \left(\frac{\kappa\gamma_T\Delta\mathrm{T}}{4} \right)^2 \left(\sqrt{D} + \frac{\kappa - 1}{\sqrt{D}} \right)^{-4}. \tag{2.111}$$

As in the previous two cases, these are the same quantities as those derived by Dietzel and Troian [8–10], expressed in nondimensional terms. The dimensional quantities will be presented in Sec. 2.3.4 with the results from the other two models.

2.3.4 Summary of Dimensional Linear Stability Predictions

After completion of the derivations for each model and computation of the predictions for K_o and β_o for each model, these quantities are converted to their dimensional analogs: the dimensional growth rates, b, and the dimensional wavelengths, λ_o. This

Table 2.1: Dimensional wavelengths and growth rates for each proposed model

Wavelength	**Growth Rate**
$\frac{\lambda_o^{\text{SC}}}{2\pi h_o} = \sqrt{\frac{2\varepsilon_o\varepsilon_p^2\gamma}{\sigma^2 h_o D^2}}\left(D+\frac{1}{\varepsilon_p}-1\right)^{3/2}$	$b_o^{\text{SC}} = \frac{\sigma^4 h_o D^4}{12\mu\gamma\varepsilon_o^2\varepsilon_p^4 h_o^3}\left(D+\frac{1}{\varepsilon_p}-1\right)^{-6}$
$\frac{\lambda_o^{\text{AP}}}{2\pi h_o} = \sqrt{\frac{\gamma u_p}{Q(1-\kappa)k_a\Delta\text{T}}}\,(D+\kappa-1)$	$b_o^{\text{AP}} = \frac{[Q(1-\kappa)k_a\Delta\text{T}]^2}{3\mu\gamma u_p^2 h_o}\,(D+\kappa-1)^{-4}$
$\frac{\lambda_o^{\text{TC}}}{2\pi h_o} = \sqrt{\frac{4\gamma}{3\kappa\gamma_{\text{T}}\Delta\text{T}}}\left(\sqrt{D}+\frac{(\kappa-1)}{\sqrt{D}}\right)$	$b_o^{\text{TC}} = \frac{3\,(\kappa\gamma_{\text{T}}\Delta\text{T})^2}{16\mu\gamma h_o}\left(\sqrt{D}+\frac{(\kappa-1)}{\sqrt{D}}\right)^{-4}$

will remove any ambiguity in the choice of characteristic scales from Sec. 2.2 and allow different functional dependencies to be elucidated more easily. Using Eq. (2.46) and Eq. (2.47), the dimensional quantities are

$$\lambda = \frac{2\pi L}{K}, \tag{2.112}$$

$$b = \frac{\beta u_c}{L}. \tag{2.113}$$

This can be done readily for each model and the resulting expressions are summarized in Table 2.1. These expressions will be used extensively throughout Ch. 3, Ch. 4, and Ch. 5.